Research Report

Model Representation of Multi-cyclic Phenomena using Role State Variables: Model Based Fast Idling Control of SI Engine

Tomohiko Jimbo and Yoshikazu Hayakawa

Report received on Dec. 13, 2010

ABSTRACT The present paper describes a model representation of multi-cyclic phenomena for a multi-cylinder engine system. The model is simplified for implementation as a practical engine controller. The simplified model with physically meaningful variables can be used in design considering practical objectives and constraints more effectively. The proposed approach consists of two steps. First, an approximate analytical discrete crank angle model (i.e., a periodically time-varying state space model) is derived from the conservation laws. Second, the concept of role state variables is proposed to transform the periodically time-varying state space model into a time-invariant state space model. The stabilizability and optimality of the time-invariant state space model imply those of the periodically time-varying state space model. The time-invariant state space model is used to design cold start feedforward and feedback controllers.

KEYWORDS SI engine, Modeling, Periodic system, Role state variable, Physical-model-based control

1. Introduction

As the regulation of automotive performance becomes increasingly strict, the development of a high-efficiency and zero-emissions powertrain has become crucial. However, it is feared that conventional development techniques will exponentially increase the man-hours required for engine control design. In order to solve this problem, the powertrain should be controlled electronically with high performance and concisely, and model-based development should be realized as soon as possible.

The engine control system is redundant because the torque is controlled by multiple inputs, such as throttle angle, fuel injection quantity, and spark timing. These inputs have a time-delay. Specifically, in the port-injection engine, the fuel injection quantity has a delay of one cycle. Moreover, the system has both time-dependent and crank angle-dependent dynamics, that is, a continuous time nonlinear phenomenon in each cylinder is switched by discrete valve opening and closing events. In addition, the system is multi-cyclic, that is, the intake, combustion (compression / expansion), and exhaust strokes are repeated cyclically in each cylinder, where the combustion stroke does not occur simultaneously in multiple cylinders.

In current engine control design, the main control method is based on maps and if-then rules and makes use of the experience of experts. However, in the design and verification processes for a new engine, this requires a great deal of time and patience.

Recently, many model based design methodologies have been proposed; for example,[1-11] for idle speed control,[12-21] for air-fuel ratio. Literatures for automotive and engine control have also been published.[22,23] Nevertheless, these methodologies combine use of partial physical models, polynomial expressions, and tables or approximate a objective input-output relation by ARX and dead time. Those are not physical models of whole engine systems. Therefore, these methodologies must treat engine systems as cooperation systems or switched systems. As a result, the analysis of the control system and the optimality could not be discussed sufficiently, because, in these methodologies, the inputs are calculated without consideration of the interactions among all of the state variables in the engine.

The present study proposes a model representation of multi-cyclic phenomena for multi-cylinder engine systems. Section 2 briefly introduces the SICE benchmark model.

Section 3 describes a method of deriving a simple model, which is periodically time-varying, for an engine system with complicated physical phenomena. We also introduce the concept of role state variables, by which the derived model can be transformed into a time-invariant state space model, and discuss the stabilizability of those models. Using the time-

Reprinted from SICE Journal of Control, Measurement, and System Integration, Vol.1, No.4, pp.320-328, Copyright 2008, with permission from the Society of Instrument and Control Engineers.

invariant state space model, optimal design examples of cold start feedforward and feedback control are demonstrated in Section 4, and Section 5 describes a numerical experiment. Finally, Section 6 presents the conclusions of the present study.

2. Benchmark model

The SICE Research Committee on Advanced Control of Engines has provided a SICE benchmark model (benchmark model) and has set the cold start control as a benchmark problem.[24]

Figure 1 shows the benchmark model, a V6 spark ignition engine, which is composed of six submodels: an air model, a fuel model (called PR model), a cylinder model, a valve-temperature model, a port-temperature model, and a piston-crank model. These models are expressed according to the following fundamental equations:

Gas equation:

$$\begin{cases} P_a V_a = M_a R T_a \\ P_{cj} V_{cj} = M_{cj} R T_{cj} \end{cases} \quad \cdots\cdots\cdots\cdots\cdots (1)$$

Mass conservation:

$$\begin{cases} \dfrac{dM_a}{dt} = m_t - \sum_{j=1}^{6} m_{ivj} \\ \dfrac{dM_{cj}}{dt} = m_{ivj} - m_{evj} \end{cases} \quad \cdots\cdots\cdots\cdots\cdots (2)$$

Energy conservation:

$$\begin{cases} \dfrac{d(M_a C_{va} T_a)}{dt} = m_t C_{po} T_o - \sum_{j=1}^{6} m_{ivj} C_{pa} T_a \\ \dfrac{d(M_{cj} C_{vcj} T_{cj})}{dt} = m_{ivj} C_{pa} T_a - m_{evj} C_{pcj} T_{cj} \\ \qquad\qquad -P_{cj} \dfrac{dV_{cj}}{dt} + q_{wj} + q_{bj} \\ \dfrac{dT_{vj}}{dt} = H_3 q_{wj} - H_4 (T_{vj} - T_o) \\ \dfrac{dT_{pi}}{dt} = \sum_{j \in J_i} (H_1 q_{wj} - H_2 (T_{pi} - T_o)) \end{cases} \quad \cdots\cdots\cdots\cdots\cdots (3)$$

Translation and rotation equations of motion (Piston-crank dynamics):

$$\begin{cases} I \dfrac{d^2 q}{dt^2} = \tau - B^T(q) \lambda \\ B(q) \dfrac{dq}{dt} = 0 \end{cases} \quad \cdots\cdots\cdots\cdots\cdots (4)$$

Fuel behavior model:

$$\begin{cases} \dfrac{dF_{wvj}}{dt} = X_{vj} f_{inj,j} - Y_{vj} F_{wvj} \\ \dfrac{dF_{wpj}}{dt} = X_{pj} f_{inj,j} - Y_{pj} F_{wpj} \\ f_{cj} = (1 - X_{vj} - X_{pj}) f_{inj,j} \\ \qquad + Y_{vj} F_{wvj} + Y_{pj} F_{wpj} \end{cases} \quad \cdots\cdots\cdots\cdots\cdots (5)$$

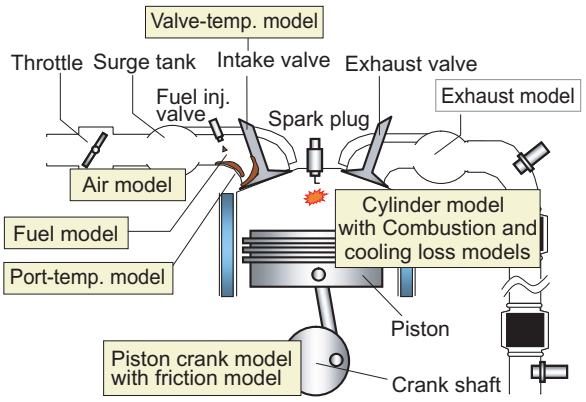

Fig. 1 Benchmark model.

where

P_a, P_{cj} : pressures in the surge tank and $\#j$ cylinder

V_a, V_{cj} : volumes in the surge tank and $\#j$ cylinder

M_a, M_{cj} : masses in the surge tank and $\#j$ cylinder

T_a, T_{cj} : temperatures in the surge tank and $\#j$ cylinder

R : gas constant

T_{pi} : temperature of intake ports set up of $\#i$ bank

T_{vj} : temperature of $\#j$ intake valve

T_o : temperature of outer air

m_t : flow of throttle

m_{ivj}, m_{evj} : flows of $\#j$ intake and exhaust valve

C_{va} : isovolumetric specific heat in the surge tank

C_{vcj} : isovolumetric specific heat in $\#j$ cylinder

C_{pa} : isobaric specific heat in the surge tank

C_{pcj} : isobaric specific heat in $\#j$ cylinder

C_{po} : isobaric specific heat of outer air

q_{bj} : combustion energy of $\#j$ cylinder

q_{wj} : cooling loss of $\#j$ cylinder

H_1, H_2, H_3, H_4 : heat transfer coefficients

q : state vector of pistons' positions and crank angle θ

I : matrix of inertia and mass

τ, λ : force and Lagrange multipliers

B : constraint space

$f_{inj,j}$: fuel flow of $\#j$ fuel injection valve

F_{wvj} : fuel quantity adhering to $\#j$ intake valve

F_{wpj} : fuel quantity adhering to $\#j$ intake port

f_{cj} : fuel flow into $\#j$ cylinder

X, Y : fuel parameters depending on T_{pi}, T_{vj}, M_{cj}, and engine speed $\omega (= d\theta/dt)$,

and the suffixes mean as follows: $j \in \{1, 2, \cdots, 6\}$: cylinder's number, $i \in \{1, 2\}$: bank's number, $J_1 = \{1, 3, 5\}$, $J_2 = \{2, 4, 6\}$. Note that the cylinder model includes combustion and cooling loss, and the port-temperature model expresses the temperatures of the left and right banks. In addition, the exhaust model is approximated in the atmosphere.

The benchmark model has 13 control inputs: one throttle angle, six fuel injection quantities, six spark timings, and two outputs: engine speed and throttle flow.

3. Modeling

The benchmark model is complex, where both time-dependent and crank angle-dependent dynamics exist over six cylinders. Therefore, a simplified model is needed for a practical controller design from the viewpoint of computational load.

Moreover, it is important to maintain the state variables to be physically meaningful in this model reduction process, considering the practical objectives and constraints more effectively. Here, we will choose the sampling points based on the crank angle to derive a simplified discrete crank angle model as follows.

1st step A set of nonlinear differential equations Eqs. (1)-(5) are solved by approximate analytical techniques to obtain the state variables at each sampling point. Thus, a nonlinear, periodically time-varying state space model is derived.

2nd step Using the new concept of role state variables, the periodically time-varying state space model is transformed into a time-invariant state space model.

3. 1 Sampling point and state variable

The engine system switches the strokes of intake, combustion and exhaust by opening and closing of intake and exhaust valves. We propose that all of the states are calculated at the end of each stroke (switching point) and at the middle of each stroke (middle point) for six cylinders. **Figure 2** shows the proposed sampling points "k". Therefore, one cycle, i.e., 720 crank angle [degCA] is divided into six sampling points, each of which contains three switching points and three middle points. Note that the discrete crank angle model is discretized approximately every 120 degCA, not precisely every 120 degCA, because these sampling points do not occur at strictly the same time.

The discrete crank angle model has 35 state variables: seven masses and seven pressures in the surge tank and each cylinder, engine speed, eight temperatures of the valve of each cylinder and of the left and right banks, 12 fuel amounts adhering to the valve of each cylinder, and the port of each cylinder.

3. 2 Periodically time-varying state space model

It is difficult to obtain the exact behaviors at each sampling point because the behaviors are subject to the nonlinear differential equations Eqs. (1)-(5). Therefore, we derive a periodically time-varying state space model using approximate analytical techniques as below:

(a) The masses and pressures in the surge tank and each cylinder during the intake stroke and the exhaust stroke are obtained from the gas equation

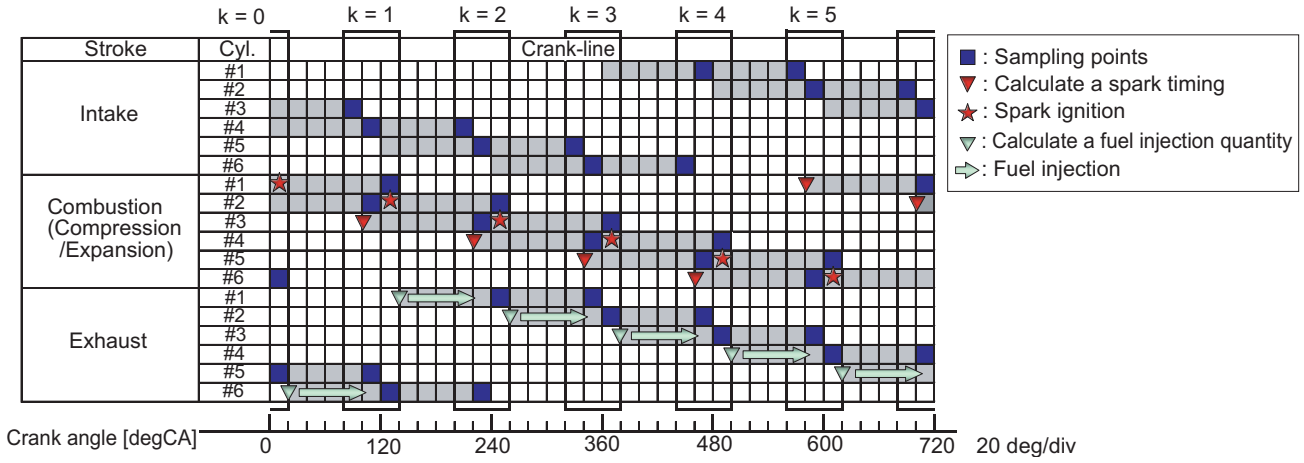

Fig. 2 Sampling points.

Eq. (1) and the conservation laws Eqs. (2) and (3) using stationary approximation at every sampling point. Note that, for six cylinders, the derived model can strictly distinguish the case of two cylinders at the intake (exhaust) stroke at the same time from that of one cylinder at the intake (exhaust) stroke.

(b) The mass and pressure in each cylinder and the piston work of each cylinder during the combustion stroke are obtained from the gas equation Eq. (1) and the conservation laws Eqs. (2) and (3) using the approximated cooling loss model. Note that mass and pressure at the opening of the exhaust valve and the piston work are expressed using only the states at the closing of the intake valve without using the states under combustion.

(c) The square of engine speed is convenient for approximating analytical techniques for Lagrange equations Eq. (4) with constraints, which express the reciprocating dynamics of the six pistons, the rotational dynamics of the crank, and their interlock.

(d) The temperature of the valve of each cylinder and the temperature of the left and right banks are derived from the conservation law Eq. (3) using approximate analytical techniques for the cooling loss model and integral terms. Note that the valve temperature at the opening of the exhaust valve is expressed using only the states at the closing of the intake valve without using the valve temperature under combustion.

(e) The fuel model is easy to discretize from the original model Eq. (5) in the benchmark model as follows: for $\#j_{eE}(k)$ cylinder at the end of exhaust stroke (eE) at sampling point k,

$$\begin{aligned} F_{wvj}(k+1) &= p_v(k)F_{wvj}(k) + r_v(k)\hat{u}_f(k) \\ F_{wpj}(k+1) &= p_p(k)F_{wpj}(k) + r_p(k)\hat{u}_f(k) \\ \hat{F}_c(k) &= (1 - r_v(k) - r_p(k))\,\hat{u}_f(k) \\ &\quad + (1 - p_v(k))\,F_{wvj}(k) + (1 - p_p(k))\,F_{wpj}(k) \end{aligned} \quad \cdots\cdots\cdots\cdots (6)$$

where $\hat{u}_f(\hat{k})$ is the fuel injection quantity of $\#j_{eE}(k)$ cylinder, $F_c(k)$ is the fuel quantity into $\#j_{eE}(k)$ cylinder. And then p_v, r_v, p_p, and r_p are easily derived from fuel parameters X, Y, and sampling time.

3. 2. 1 Masses and pressures during intake stroke

Now we will describe briefly the intake stroke in the process (a). The intake stroke from sampling points k to $k+1$ consists of two phases. For six cylinders, in the first phase of $[t_{s1}, t_{f1}]$ two cylinders' (e.g., $\#j_1$ and $\#j_2$) valves are open, and in the second phases of $[t_{s2}, t_{f2}]$ with $t_{s2} = t_{f1}$, one cylinder's (e.g., $\#j_1$) valve is open, the other cylinders' (including $\#j_2$) valves are close. Note that the state variables in the intake stroke are composed of the masses and pressures in the surge tank, $\#j_1$, and $\#j_2$ cylinder. Furthermore, the state variables at the sampling point k correspond with those at $t = t_{s1}$, and the state variables at the sampling point $k+1$ correspond with those at $t = t_{f1}$ for $\#j_2$ cylinder and at $t = t_{f2}$ for the surge tank and $\#j_1$ cylinder.

From Eqs. (1), (2), and the first and second equations of Eq. (3) where, for $j = j_1, j_2$, the flow of exhaust valve $m_{ev j} = 0$, the combustion energy $q_{bj} = 0$, it is easy to see that the following equations hold

$$\int dM_a = \int m_t dt - \sum_{j\in I_i} \int dM_{cj} \quad \cdots\cdots\cdots\cdots (7)$$

$$\begin{aligned} \int \frac{d(P_a V_a)}{\kappa_a - 1} &= \int \frac{\kappa_o P_o}{(\kappa_o - 1)\rho_o} m_t dt \\ &\quad + \sum_{j\in I_i} \left\{ - \int P_{cj} dV_{cj} - \int \frac{d(P_{cj}V_{cj})}{\kappa_{cj} - 1} + \int q_{wj} dt \right\} \end{aligned} \quad \cdots\cdots\cdots\cdots\cdots (8)$$

where $i \in \{1, 2\}$ denotes the phase, $I_1 = \{j_1, j_2\}$, $I_2 = \{j_1\}$, P_0 and ρ_0 are pressure and density of outer air. And then κ_a, κ_{cj}, κ_0 are specific heat ratios in the surge tank and in $\#j$ cylinder, and of outer air, respectively. Note that $C_{v*} = R/(\kappa_* - 1)$, $C_{p*} = \kappa_* R/(\kappa_* - 1)$ with $* = a, cj, o$.

By an experimental observation that the pressure of cylinder $P_{cj}(t)$ for $j \in I_i$ converges immediately after opening the intake valve, we suppose that $P_{cj}(t) = P_{cj}(t_{fi})$ for $t \in (t_{si}, t_{fi}]$. Besides, it is assumed that in Eq. (8), $q_{wj} = 0$ and $\kappa_0 = \kappa_a = \kappa_{cj} = \kappa =$ (: constant.), in the nozzle flow function m_t, the throttle angle $u_t(t) = u_t(t_{s1})$ and $P_a(t) = P_a(t_{s1})$ for $t \in [t_{s1}, t_{f2})$. As a result, it is obtained that

$$\begin{aligned} &M_a(t_{fi}) - M_a(t_{si}) \\ &\quad = M_{ti} - \sum_{j\in I_i} \{M_{cj}(t_{fi}) - M_{cj}(t_{si})\} \end{aligned} \quad \cdots\cdots (9)$$

$$\begin{aligned} &P_a(t_{fi})V_a(t_{fi}) - P_a(t_{si})V_a(t_{si}) \\ &\quad = \frac{\kappa P_o}{\rho_o} M_{ti} \\ &\qquad - (\kappa - 1) \sum_{j\in I_i} [P_{cj}(t_{fi})\{V_{cj}(t_{fi}) - V_{cj}(t_{si})\}] \\ &\qquad - \sum_{j\in I_i} \{P_{cj}(t_{fi})V_{cj}(t_{fi}) - P_{cj}(t_{si})V_{cj}(t_{si})\} \end{aligned} \quad \cdots\cdots\cdots\cdots (10)$$

where

$$\begin{aligned} M_{ti} &= \int_{t_{si}}^{t_{fi}} m_t dt \\ &= A_t \left(1 - cos\left(\frac{\pi u_t(t_{s1})}{180}\right)\right) \Psi(P_a(t_{s1}))(t_{fi} - t_{si}), \end{aligned} \quad \cdots\cdots\cdots\cdots (11)$$

A_t is constant, and Ψ is a nozzle flow function.

From Eqs. (9) and (10), by using the following assumptions, which are from experimental observations,

$$\frac{M_a(t_{f1})}{V_a} = \frac{M_{cj_1}(t_{f1})}{V_{cj_1}(t_{f1})} = \frac{M_{cj_2}(t_{f1})}{V_{cj_2}(t_{f1})}$$
$$\frac{M_a(t_{f2})}{V_a} = \frac{M_{cj_1}(t_{f2})}{V_{cj_1}(t_{f2})}$$
$$P_a(t_{f1}) = P_{cj_1}(t_{f1}) = P_{cj_2}(t_{f1})$$
$$P_a(t_{f2}) = P_{cj_1}(t_{f2})$$

and by using the following facts, derived from $t_{s2} = t_{f1}$,

$$M_a(t_{s2}) = M_a(t_{f1}), \qquad M_{cj_1}(t_{s2}) = M_{cj_1}(t_{f1})$$
$$P_a(t_{s2}) = P_a(t_{f1}), \qquad P_{cj_1}(t_{s2}) = P_{cj_1}(t_{f1}),$$

we can express the masses and pressures in the surge tank and cylinders for the intake stroke, which are a part of Eq. (24),

$$x_{m,in}(k+1) = A_{m,in}\, x_{m,in}(k) + B_{m,in}\, M_t(k)$$
$$x_{p,in}(k+1) = A_{p,in}\, x_{p,in}(k) + B_{p,in}\, M_t(k) \quad \cdots\cdots (12)$$

where $A_{m,in} \in \mathrm{R}^{3\times3}$, $B_{m,in} \in \mathrm{R}^{3\times2}$, $A_{p,in} \in \mathrm{R}^{3\times3}$, $B_{p,in} \in \mathrm{R}^{3\times2}$ are constant matrices, and

$$x_{m,in}(k+1) = \begin{bmatrix} M_a(k+1) \\ M_{cj_1}(k+1) \\ M_{cj_2}(k+1) \end{bmatrix} = \begin{bmatrix} M_a(t_{f2}) \\ M_{cj_1}(t_{f2}) \\ M_{cj_2}(t_{f1}) \end{bmatrix}$$

$$x_{m,in}(k) = \begin{bmatrix} M_a(k) \\ M_{cj_1}(k) \\ M_{cj_2}(k) \end{bmatrix} = \begin{bmatrix} M_a(t_{s1}) \\ M_{cj_1}(t_{s1}) \\ M_{cj_2}(t_{s1}) \end{bmatrix}$$

$$x_{p,in}(k+1) = \begin{bmatrix} P_a(k+1) \\ P_{cj_1}(k+1) \\ P_{cj_2}(k+1) \end{bmatrix} = \begin{bmatrix} P_a(t_{f2}) \\ P_{cj_1}(t_{f2}) \\ P_{cj_2}(t_{f1}) \end{bmatrix}$$

$$x_{p,in}(k) = \begin{bmatrix} P_a(k) \\ P_{cj_1}(k) \\ P_{cj_2}(k) \end{bmatrix} = \begin{bmatrix} P_a(t_{s1}) \\ P_{cj_1}(t_{s1}) \\ P_{cj_2}(t_{s1}) \end{bmatrix}$$

$$M_t(k) = \begin{bmatrix} M_{t2}(P_a(k), \Omega(k), u_t(k)) \\ M_{t1}(P_a(k), \Omega(k), u_t(k)) \end{bmatrix}$$

$$u_t(k) = u_t(t_{s1}).$$

Next the explanation for the exhaust stroke in (a) can be derived as well, but in this study, cylinder model for the exhaust stroke is also approximated in the atmosphere as well as exhaust model.

3. 2. 2 Mass and pressure, and piston work during combustion stroke

The detail explanation is omitted here because of the space limitations.

As a result, in (b), by using each second equation of Eqs. (1), (2), and (3), the explanations of the mass and the pressure at the end of combustion stroke, and the piston work during the combustion stroke can be represented as follows:

for $\#j \in j_{mC}(k)$ cylinder at the middle of combustion (mC) at sampling point k,

$$M_{cj}(k+1) = M_{cj}(k-1) \quad \cdots\cdots (13)$$

$$P_{cj}(k+1) = a_{p1}P_{cj}(k-1) + a_{p2}M_{cj}(k-1)T_{pi}(k) + g_p(\hat{u}_s(k))\hat{F}_c(k)H_f(\hat{\alpha}_c(k)) \quad \cdots\cdots (14)$$

$$W_{cmb,j}(k) = \int_{t_{eI}}^{t_{eC}} P_{cj}dV_{cj} = a_{w1}P_{cj}(k-1) + a_{w2}M_{cj}(k-1)T_{pi}(k) + g_w(\hat{u}_s(k))\hat{F}_c(k)H_f(\hat{\alpha}_c(k)) \quad \cdots\cdots (15)$$

where sampling points k+1, k, k–1 respond times at the end of combustion (t_{eC}), at the middle of combustion (t_{mC}), and at the end of intake (t_{eI}), respectively. And then a_{p1}, a_{p2}, a_{w1}, and a_{w2} are constants. $\hat{u}_s(k)$ and $\hat{F}_c(k)$ and $\hat{a}_c(k)$ are spark timing and fuel quantity, and air-fuel ratio, respectively, for the cylinder at the middle of combustion, at sampling point k. g_p and g_w are functions of spark timing, H_f is the lower heating value as a function of air-fuel ratio. Note that, for convenience sake,

$$P_{cj}(k) = P_{cj}(k-1) \quad \cdots\cdots (16)$$

because $P_{cj}(k)$ is not needed for calculation of $P_{cj}(k+1)$. And, In facts,

$$M_{ci}(k) = M_{ci}(k-1) \quad \cdots\cdots (17)$$

3. 2. 3 Engine speed

As a result, in (c), by using Eq. (4), the explanation of the square of engine speed $\Omega(=\omega^2)$ can be represented by

$$\Omega(k+1) = \Omega(k) + a_\Omega \left(W(k) - \frac{2\pi}{3}\tau_f(k) \right) \quad \cdots (18)$$

where, for six cylinders,

$$W(k) = W_{cmb,j_{mC}(k)}(k) + a_{eC}P_{cj_{eC}(k)}(k) + a_{mE}P_{cj_{mE}(k)}(k) + a_{eE}P_{cj_{eE}(k)}(k) + a_{mI}P_{cj_{mI}(k)}(k),$$

$j_{mI}(k)$, $j_{eE}(k)$, $j_{mE}(k)$, $j_{eC}(k)$, and $j_{mC}(k)$ are the cylinders' numbers at the middle of intake stroke (mI), at the end of exhaust stroke (eE), at the middle of exhaust stroke (mE), at the end of combustion stroke (eC), and at the middle of combustion stroke (mC), respectively, at sampling point k. And a_Ω, a_{mI}, a_{eE}, a_{mE}, and a_{eC} are constants.

3. 2. 4 Temperature of each valve and each bank

As a result, in (d), by using the third equation of Eq. (3), the explanation of the temperature of each valve for six cylinders can be represented as follows:

1) for $\#j \in \{j_{eC}(k), j_{mE}(k), j_{eE}(k), j_{mI}(k)\}$ cylinder

$$T_{vj}(k+1) = e^{\frac{a_{tv1}}{\sqrt{\Omega(k)}}} T_{vj}(k) + \left(1 - e^{\frac{a_{tv1}}{\sqrt{\Omega(k)}}}\right) \times \left(a_{tv2}\sqrt{\Omega(k)}\left(P_{cj}(k) - \frac{M_{cj}(k)RT_{pi}(k)}{V_{cj}(k)}\right) + T_o\right) \quad \cdots\cdots (19)$$

2) for $\#j \in \{j_{mC}(k)\}$ cylinder

$$T_{vj}(k+1) = e^{\frac{a_{tv3}}{\sqrt{\Omega(k)}}} T_{vj}(k-1) + \left(1 - e^{\frac{a_{tv3}}{\sqrt{\Omega(k)}}}\right) T_o + a_{tv4}\left(X_{cmb,j}(k) - a_{vinv} M_{cj}(k-1) RT_{pi}(k)\right) \quad \cdots\cdots (20)$$

where

$$X_{cmb,j}(k) = a_{x1} P_{cj}(k-1) + a_{x2} M_{cj}(k-1) T_{pi}(k) + g_x(\hat{u}_s(k)) \hat{F}_c(k) H_f(\hat{\alpha}_c(k)),$$

a_{tv1}, a_{tv2}, a_{tv3}, a_{tv4}, a_{vinv}, a_{x1}, and a_{x2} are constants, g_x is a function of spark timing $\hat{u}_s$. Note that, as well as Eqs. (14) and (15), Eq. (16) is used, Eq. (17) is true. And for the same reason with P_{cj} of Eq. (16),

$$T_{vj}(k) = T_{vj}(k-1). \quad \cdots\cdots (21)$$

Next, in (d), by using the fourth equation of Eq. (3), the explanation of the temperature of each bank for six cylinders can be represented as follows: recalling that $J_1 = \{1, 3, 5\}$, $J_2 = \{2, 4, 6\}$,

1) for $\#i$ bank with $J_i = \{j_{eC}(k), j_{eE}(k), j_{eI}(k)\}$

$$T_{pi}(k+1) = e^{\frac{a_{tp1}}{\sqrt{\Omega(k)}}} T_{pi}(k) + \left(1 - e^{\frac{a_{tp1}}{\sqrt{\Omega(k)}}}\right) \times \left(a_{tp2}\sqrt{\Omega(k)} \sum_{j \in \{j_{eC(k)}, j_{eE(k)}\}} \left(P_{cj}(k) - \frac{M_{cj}(k)RT_{pi}(k)}{V_{cj}(k)}\right) + T_o\right) \quad \cdots\cdots (22)$$

2) for $\#i$ bank with $J_i = \{j_{mC}(k), j_{mE}(k), j_{mI}(k)\}$

$$T_{pi}(k+1) = e^{\frac{a_{tp1}}{\sqrt{\Omega(k)}}} T_{pi}(k) + \left(1 - e^{\frac{a_{tp1}}{\sqrt{\Omega(k)}}}\right) \times \left(a_{tp2}\sqrt{\Omega(k)} \sum_{j \in \{j_{mE(k)}, j_{mI(k)}\}} \left(P_{cj}(k) - \frac{M_{cj}(k)RT_{pi}(k)}{V_{cj}(k)}\right) + T_o\right) + e^{-\frac{a_{tp1}}{\sqrt{\Omega(k)}}} a_{tp3}\left(X_{cmb,j_{mC(k)}}(k) - a_{vinv} M_{cj_{mC(k)}}(k-1) RT_{pi}(k)\right) \quad \cdots\cdots (23)$$

where $j_{eI}(k)$ is the cylinder's number at the end of intake stroke (eI) at sampling point k. And a_{tp1}, a_{tp2}, and a_{tp3} are constants. In fact, Eq. (17) is true. Here $M_{cjmC(k)}(k) = M_{cjmC(k)}(k-1)$.

3. 2. 5 Integrated mode

From combining each discrete crank angle model Eqs. (12)-(14), (16)-(23), and (6), as outlined in (a), (b), (c), (d), and (e), we obtain the following periodically time-varying state space model,

$$\begin{aligned} x(k+1) &= f_{\overline{k}}(x(k), u(k)) \\ y(k) &= h(x(k)) \end{aligned} \quad \cdots\cdots (24)$$

where the notations are used as follows:

$\overline{k} = k \bmod 6$

$x = [x_c{}^T \; F_w{}^T \; z^T]^T \in R^{42}$: state variable

$x_c = [M^T \; P^T \; \Omega \; T_v{}^T \; T_p{}^T]^T \in R^{23}$

$M = [M_a \; M_{c1} \; \ldots \; M_{c6}]^T \in R^7$

$P = [P_a \; P_{c1} \; \ldots \; P_{c6}]^T \in R^7$

$T_v = [T_{v1} \; \ldots \; T_{v6}]^T \in R^6$, $T_p = [T_{p1} \; T_{p2}]^T \in R^2$

$F_w = [F_{wv}{}^T \; F_{wp}{}^T]^T \in R^{12}$

$F_{wv} = [F_{wv1} \; \ldots \; F_{wv6}]^T \in R^6$

$F_{wp} = [F_{wp1} \; \ldots \; F_{wp6}]^T \in R^6$

$z = [z_c{}^T \; z_f{}^T]^T \in R^7$: unit delay

$z_c = [u_t \; \hat{u}_s \; \hat{F}_c]^T \in R^3$, $z_f \in R^4$

$y = [\Omega \; m_t]^T \in R^2$: output

$u = [u_t \; u_s{}^T \; u_f{}^T]^T \in R^{13}$: real input

$u_s = [u_{s1} \; \ldots \; u_{s6}]^T \in R^6$, $u_f = [u_{f1} \; \ldots \; u_{f6}]^T \in R^6$.

Figure 3 shows the entire model of Eq. (24). Note that the total delay is five samples in the fuel model because the torque is generated one cycle after the fuel injection quantity is specified as the opening exhaust valve. The delays of the throttle angle and the spark timing indicate that throttle opening and spark are executed one sample after specified. Furthermore, the torque, the thermal efficiency, and the specific fuel consumption can also be expressed by the state variable x and the input u.

Figure 4 shows the validation of the obtained model (Fig. 3). These errors are mainly caused by approximating the cooling loss. Notice that the computational load of the obtained model is less than 1/100 that of the benchmark models Eqs. (1)-(5).

3. 3 Time-invariant state space model

3. 3. 1 Role state variable

Table 1(a) summarizes Fig. 2, showing the relation among the cylinder number, the sampling point, and the

types of strokes. In Table 1(a), ξ_j is the state variables of mass, pressure, and valve temperature in the #j cylinder. It is easy to see that the state transition function at sampling points k to k+1 is different from that at sampling points k+1 to k+2, because the stroke of ξ_j at sampling points k to k+1 is different from that at sampling points k+1 to k+2. This is why Eq. (24) is time-varying and periodical.

Next, we introduce a new state variable. The relation shown in Table 1(b) is the same as that shown in Table 1(a), except with respect to how to choose the state variables. In Table 1(b), the state variable $\hat{\xi}_1$ is defined in terms of the mass, pressure, and valve temperature at the middle of the combustion stroke (mC). Similarly, state variables $\hat{\xi}_2$ to $\hat{\xi}_6$ are defined as mass, pressure, and valve temperature under the corresponding strokes. We define these state variables $\hat{\xi}$ as role state variables. Note that role state variables are continuous values.

The state transition function of $\hat{\xi}_i$ at sampling points k to k+1 is the same as that at sampling points k+1 to k+2 because the state variable $\hat{\xi}_i$ is always in the same stroke. Therefore, the periodically time-varying state space model of Eq. (24) can be transformed into a time-invariant state space model if the role state variables are used.

When the role state variables are used, there exist only three inputs: the spark timing, the fuel injection quantity, and the throttle angle. We refer to these inputs as role inputs. The role input of spark timing is a reduced input from six spark timings of all of the

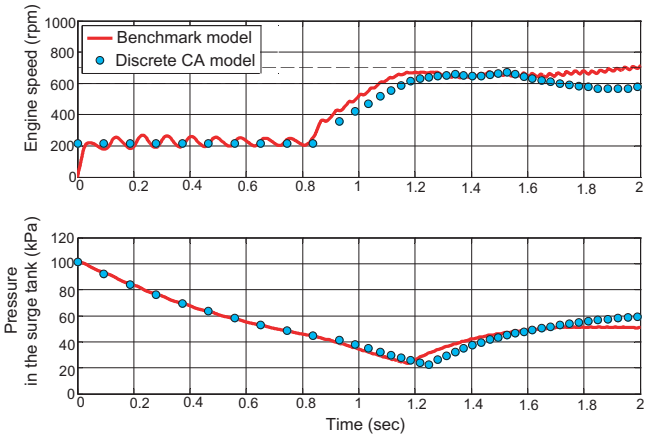

Fig. 4 Validation.

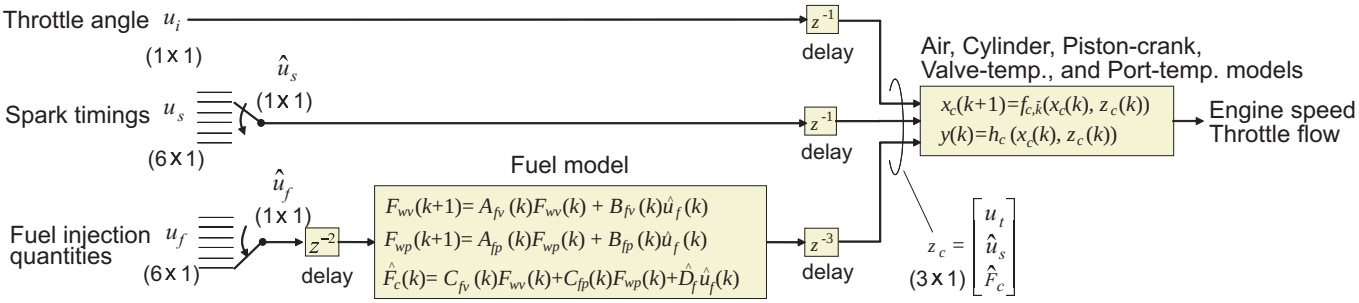

Fig. 3 Periodically time-varying state space model.

Table 1 Relation between state variables and role state variables:
mI: Middle of Intake stroke, mC: Middle of Combustion stroke, mE: Middle of Exhaust stroke,
eI: End of Intake stroke, eC: End of Combustion stroke, eE: End of Exhaust stroke, #: cylinder number

(a) State variable

State Variables \ Sampling Point	0	1	2	3	4	5	6	7	...
ξ_1 at #1	mC	eC	mE	eE	mI	eI	mC	eC	...
ξ_2 at #2	eI	mC	eC	mE	eE	mI	eI	mC	...
ξ_3 at #3	mI	eI	mC	eC	mE	eE	mI	eI	...
ξ_4 at #4	eE	mI	eI	mC	eC	mE	eE	mI	...
ξ_5 at #5	mE	eE	mI	eI	mC	eC	mE	eE	...
ξ_6 at #6	eC	mE	eE	mI	eI	mC	eC	mE	...

(b) Role state variable

Role State Variables \ Sampling Point	0	1	2	3	4	5	6	7	...
$\hat{\xi}_1$ at mC	#1	#2	#3	#4	#5	#6	#1	#2	...
$\hat{\xi}_2$ at eI	#2	#3	#4	#5	#6	#1	#2	#3	...
$\hat{\xi}_3$ at mI	#3	#4	#5	#6	#1	#2	#3	#4	...
$\hat{\xi}_4$ at eE	#4	#5	#6	#1	#2	#3	#4	#5	...
$\hat{\xi}_5$ at mE	#5	#6	#1	#2	#3	#4	#5	#6	...
$\hat{\xi}_6$ at eC	#6	#1	#2	#3	#4	#5	#6	#1	...

cylinders, as well as the role input of fuel injection. Therefore, it is important to grasp the correspondence between the role inputs and the real inputs. Note that the role input of the throttle angle is equal to the real input.

Using the role state variables and the role inputs, the periodically time-varying state space model of Eq. (24) is transformed into the following time-invariant state space model,

$$\begin{aligned} \hat{x}(k+1) &= f(\hat{x}(k), \hat{u}(k)) \\ y(k) &= h(\hat{x}(k)) \end{aligned} \quad \cdots\cdots\cdots\cdots\cdots (25)$$

$$\hat{x} = [\hat{x}_c^T \ \hat{F}_w^T \ z^T]^T \in R^{42} : \text{role state variable}$$

$$\hat{x}_c = [\hat{M}^T \ \hat{P}^T \ \Omega \ \hat{T}_v^T \ \hat{T}_p^T]^T \in R^{23}$$

$$\hat{M} = [M_a \ \hat{M}_{c1} \ \ldots \ \hat{M}_{c6}]^T \in R^7$$

$$\hat{P} = [P_a \ \hat{P}_{c1} \ \ldots \ \hat{P}_{c6}]^T \in R^7$$

$$\hat{u} = [u_t \quad \hat{u}_s \quad \hat{u}_f]^T \in R^3 : \text{role input.}$$

where the notations are used as follows:

Figure 5 shows an entire model of Eq. (25).

The concept of the role state variables has been discussed here in the case of six-cylinders. Note, however, that the discussion holds for any number of cylinders. In fact, basically, we should select sampling points which are divided one cycle, i.e., 720 degCA into the number of cylinders. And then, states of divided transition are selected as role state variables with a same set of state transition functions in each sample interval.

3. 3. 2 Permutation matrix

This section clarifies the relation between the role state variables and the state variables, as well as the relation between the role inputs and the real inputs.

From the relation between the role state variables $\hat{\xi}_i$ and the state variables ξ_j in Table 1, using the following permutation matrix Q, the transformation between $\hat{\xi}(k)$ and $\xi(k)$ is given by

$$\hat{\xi}(k) = Q^{\overline{k}}\xi(k), \quad Q = \begin{bmatrix} 0_{5\times1} & I_5 \\ 1 & 0_{1\times5} \end{bmatrix} \cdots\cdots (26)$$

where $\overline{k} = k \bmod 6$. Similarly, the relation between the role inputs and the real inputs is given by

$$\hat{u}_s(k) = r_s{}^T Q^{\overline{k}} u_s(k), \quad \hat{u}_f(k) = r_f{}^T Q^{\overline{k}} u_f(k) \quad \cdots\cdots\cdots\cdots\cdots (27)$$

where $r_s = [0\ 1\ 0\ 0\ 0\ 0]^T$, $r_f = [0\ 0\ 0\ 0\ 0\ 1]^T$.

3. 3. 3 Stabilizability

We consider some linearized models around a steady state to clarify the relation between the stabilizability of the time-invariant state space model Eq. (25) with the role state variables and that of the periodically time-varying state space model Eq. (24).

Equations (28) and (29) indicates the linearized state space models derived from the periodically time-varying state space model Eq. (24) and the time-invariant state space model Eq. (25), in which Δu and $\Delta\hat{u}$, Δx and $\Delta\hat{x}$, and Δy denote the perturbations of inputs, states, and outputs, respectively, from a steady state. Here, we assume that in a steady state, the fuel quantity in a cylinder is equal to the fuel injection quantity, and thus the fuel model, the valve-temperature model, and the port-temperature model can be disregarded.

$$\begin{aligned} \Delta x(k+1) &= A(k)\Delta x(k) + B(k)\Delta u(k) \\ \Delta y(k) &= C(k)\Delta x(k) \end{aligned} \quad \cdots\cdots (28)$$

$$\begin{aligned} \Delta\hat{x}(k+1) &= \hat{A}\Delta\hat{x}(k) + \hat{B}\Delta\hat{u}(k) \\ \Delta y(k) &= \hat{C}\Delta\hat{x}(k) \end{aligned} \quad \cdots\cdots\cdots (29)$$

where

$$\Delta\hat{x}(k) = Q_x{}^{\overline{k}}\Delta x(k), \qquad A(k) = Q_x{}^{-\overline{k+1}}\hat{A}Q_x{}^{\overline{k}}$$

$$\Delta\hat{u}(k) = R_u Q_u{}^{\overline{k}}\Delta u(k), \qquad B(k) = Q_x{}^{-\overline{k+1}}\hat{B}R_u Q_u{}^{\overline{k}}$$

$$\Delta u(k) = Q_u{}^{-\overline{k}} R_u{}^T \Delta\hat{u}(k), \quad C(k) = \hat{C}Q_x{}^{\overline{k}}$$

$$Q_a = \mathrm{diag}(1, Q), \qquad Q_x = \mathrm{diag}(Q_a, Q_a, 1, I_7)$$

$$Q_u = \mathrm{diag}(1, Q, Q), \qquad R_u = \mathrm{diag}(1, r_s{}^T, r_f{}^T).$$

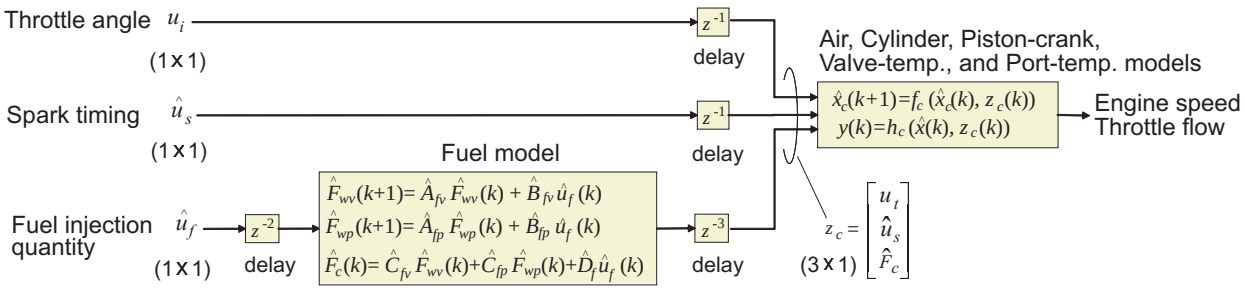

Fig. 5 Time-invariant state space model.

Theorem In Eqs. (28) and (29), the periodically time-varying state space model is stabilizable if the time-invariant state space model is stabilizable.

Proof If the time-invariant state space model is stabilizable, there exists a gain matrix $\hat{F}$ such that $\hat{A} + \hat{B}\hat{F}$ is stable.

Substituting $\Delta\hat{u}(k) = \hat{F}\Delta\hat{x}(k)$ into $\Delta u(k)$ yields $\Delta u(k) = F(k)\Delta x(k)$ where $F(k)$ is given by

$$F(k) \equiv {Q_u}^{-\overline{k}} R_u{}^T \hat{F} {Q_x}^{\overline{k}} \quad \cdots\cdots\cdots\cdots\cdots (30)$$

The periodically time-varying state space model is then given by

$$\Delta x(k+1) = \{A(k) + B(k)F(k)\}\Delta x(k) \quad \cdots\cdots (31)$$

where

$$A(k) + B(k)F(k) = {Q_x}^{-\overline{k+1}}(\hat{A} + \hat{B}\hat{F}){Q_x}^{\overline{k}} \quad \cdots (32)$$

The stability of the periodically time-varying state space model is decided according to the transition matrix from arbitrary sampling point k to sampling point k+6, i.e., by one cycle

$$\Delta x(k+6) = \Phi(k+6, k)\Delta x(k) \quad \cdots\cdots\cdots\cdots (33)$$

where from Eqs. (31) and (32), it is easy to see that

$$\Phi(k+6, k) = {Q_x}^{-\overline{k}}(\hat{A} + \hat{B}\hat{F})^6 {Q_x}^{\overline{k}} \quad \cdots\cdots\cdots (34)$$

Therefore, it is clear that $\Phi(k+6, k)$ is stable when $\hat{A}+\hat{B}\hat{F}$ is stable, which means that the theorem has been proven. □

This theorem implies that the stabilization problem of the periodically time-varying state space model can be reduced to that of the time-invariant state space model. In addition, it is easy to see that a similar theorem holds with respect to detectability. Therefore, we can use the control theory of time-invariant systems in the design of an engine feedback controller.

4. Design example

The benchmark problem mainly sets up the following control specifications.

- The engine speed, 650 ± 50 rpm, should be reached in 1.5 seconds after cold start.
- The overshoot of the engine speed should be as small as possible.
- The engine speed should converge to 650 rpm, and so the steady state of engine speed, 650 rpm should be asymptotically stable.

Figure 6 shows the design flow diagram.

1st step The sets of the steady states and inputs are obtained numerically using the nonlinear time-invariant state space model of Eq. (25) without the fuel model, the valve-temperature model, and port-temperature model, in which a set of 15 nonlinear algebraic equations $\hat{x} = f(\hat{x}, \hat{u})$ should be solved numerically with $\Omega(\in \hat{x}) = 650$ rpm.

2nd step An optimal feedforward control inputs for the 1.5 seconds after cold start is searched using Eq. (25), a performance index (square sum of the engine speed error), and some constraints (engine speed, inputs, misfire, and stall).

3rd step An LQI controller is obtained by using the linear time-invariant state space model of Eq. (29) and considering the unit delays of the inputs.

Figure 7 shows the cold start controller designed in the present study. Here $\Delta\hat{x}_r = [\Delta\hat{M}^T \ \Delta\hat{P}^T \ \Delta\Omega]^T, \in R_{15}$, $z \in R^7$ is unit delay of inputs, $\varepsilon \in R^7$ is integrator.

5. Numerical experiment

Using the benchmark model and the designed controller given in Fig. 7, numerical experiments for

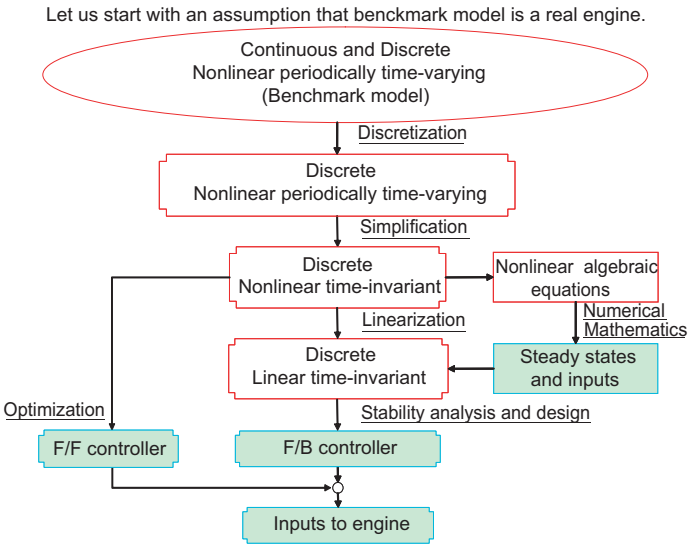

Fig. 6 Design flow diagram.

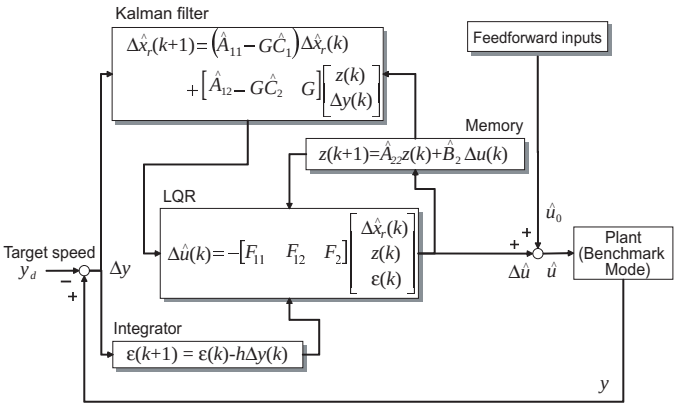

Fig. 7 Cold start controller.

cold start control were conducted. **Figure 8** shows results that satisfy the specifications of the benchmark problem. In Fig. 8, the feedback control was executed from the sixth cycle (approximately 1.8 seconds), at which time the temperatures of the valves of all of the cylinders were near steady state. Moreover, the feedforward control inputs were kept at the steady state values after this time. Note that in Fig. 8, the spark timing and the fuel injection quantity are plotted for every sample, i.e., for different cylinders.

6. Conclusions

The present paper proposes a model representation of multi-cyclic phenomena for a multi-cylinder engine system using the new concept of role state variables in order to design an optimal multiple inputs. The features of this model representation are as follows.

- The periodically time-varying state space model is equivalently transformed into the time-invariant state space model using the role state variables. This holds for any number of cylinders.
- The stabilizability of the time-invariant state space model implies the stabilizability of the periodically time-varying state space model, as well as detectability.
- The time-invariant state space model enables an optimal design for periodical engine system.
- The time-invariant state space model and the permutation matrix introduce some simplification in the program structure when the controller is implemented.

In the future, MPC will be applied explicitly to consider the constraints of inputs.

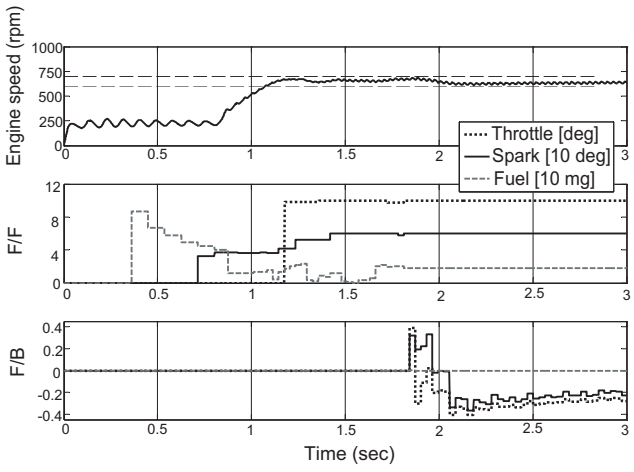

Fig. 8 Result.

References

(1) Moskwa, J. J., et al., "Automotive Engine Modeling for Real Time Control Application", *Proceedings of the 1987 American Control Conference,* (1987), pp.341-346.

(2) Nasu, M., et al., "Idle Speed Control by Nonlinear Feedback", *JSAE Review*, Vol.13, No.2 (1991), pp.54-60.

(3) Kjergaard, L., et al., "Advanced Nonliner Engine Idle Speed Control Systems", *SAE Tech. Pap. Ser.*, No.940974 (1994).

(4) Balluchi, A., et al., "Maximal Safe Set Computation for Idle Speed Control of an Automotive Engine", *Lecture Notes in Computer Science,* Vol.1790 (2000), pp.32-44.

(5) Kajitani, M., et al., "High Performance Idel Speed Control Applying the Sliding Mode Control with H Robust Hyperplane", *SAE Tech. Pap. Ser.*, No.2001-01-0263 (2001).

(6) Ganesan, S., et al., "An Idle Speed Controller Using Analytically Developed Fuzzy Logic Control Law", *SAE Tech. Pap. Ser.*, No.2002-01-0138 (2002).

(7) Singh, N., et al., "ICE Idle Speed Control Using Fuzzy Idle", *SAE Tech. Pap. Ser.*, No.2002-01-1151 (2002).

(8) Cavina, N., et al., "Model-Based Idle Speed Control for a High Performance Engine", *SAE Tech. Pap. Ser.*, No.2003-01-0358 (2003).

(9) Benvenuti, L., et al., "Individual Cylinder Characteristic Estimation for a Spark Injection Engine", *Automatica*, Vol.39, No.7 (2003), pp.1157-1169.

(10) Yasui, Y., et al., "Accurate Engine Speed Control Using Adaptive Disturbance Observer", *JSAE Tech. Pap. Ser.*, No.2004-08-0313 (2004).

(11) Higashitani, K., et al., "An Accurate Idle Speed Control for a Gasoline Engine with a Continuously Variable Valve Actuation", *SAE Tech. Pap. Ser.*, No.2007-01-1201 (2007).

(12) Inagaki, H., et al., "An Adaptive Fuel Injection Control with Internal Model in Automotive Engines", *IECON'90,* (1990), pp.78-83.

(13) Grizzle, J. W., et al., "Individual Cylinder Air-Fuel Ratio Control with a Single EGO Sensor", *IEEE Transactions on Vehicular Technology*, Vol.40, No.1 (1991), pp.280-286.

(14) Hasegawa, Y., et al., "Individual Cylinder Air-Fuel Ratio Feedback Control Using an Observer", *SAE Tech. Pap. Ser.*, No.940376 (1994).

(15) Maki, H., et al., "Real Time Engine Control Using STR in Feedback System", *SAE Tech. Pap. Ser.*, No.950007 (1995).

(16) Ohata, A., et al., "Model Based Air Fuel Ratio Control for Reducing Exhaust Gas Emissions", *SAE Tech. Pap. Ser.*, No.950075 (1995).

(17) Takahashi, S., et al., "Air-Fuel Ratio Control in Gasoline Engines Based on State Estimation and Prediction Using Dynamic Modes", *IECON Proceedings*, Vol.1 (1995), pp.217-222.

(18) Nasu, M., et al., "Model-Based Fuel Injection Control System for SI Engines", *SAE Tech. Pap. Ser.*, No.961188 (1996).
(19) Yasui, Y., et al., "Secondary O_2 Feedback Using Prediction and Identification Type Sliding Mode Control", *SAE Tech. Pap. Ser.*, No.2000-01-0936 (2000).
(20) Wendeker, M., et al., "Hybrid Air/Fuel Ratio Control Using the Adaptive Estimation and Neural Network", *SAE Tech. Pap. Ser.*, No.2000-01-1248 (2000).
(21) Hosoya, H., et al., "Development of Next-Generation Air-Fuel Ratio Control System, COSMIC", *SAE Tech. Pap. Ser.*, No.2002-01-0477 (2002).
(22) Johansson, R., et al., *Nonlinear and Hybrid Systems in Automotive Control,* (2003), Springer-Verlag London.
(23) Jurgen, R. K., *Electronic Engine Control Technologies 2nd Edition,* (2004), SAE.
(24) Ohata, A., et al., "Benchmark Problem for Automotive Engine Control", *SICE Annual Conference 2007*, (2007).

Tomohiko Jimbo
Research Fields :
- Physical modeling in engine systems
- Automotive engine control
- Model predictive control

Academic Degree : Dr. Eng.
Academic Societies :
- The Society of Instrument and Control Engineers
- Society of Automotive Engineers of Japan

Awards :
- Young Author Award, SICE, 2007
- The IFAC Congress Applications Paper Prize as one of five finalists, 2008
- Best Paper Award, SICE, 2009

Yoshikazu Hayakawa*
Research Fields :
- System and control theory
- Robot control
- Vibration control

Academic Degree : Dr. Eng.
Academic Societies :
- IEEE
- The Society of Instrument and Control Engineers
- The Institute of Systems, Control and Information Engineers
- The Japan Society of Mechanical Engineers
- The Robotics Society of Japan
- IEICE

Awards :
- Best Paper Award, SICE, 1984
- SICE Fellow, 2007
- The IFAC Congress Applications Paper Prize as one of five finalists, 2008
- Best Paper Award, SICE, 2009

*Nagoya University